T Cell Priming by Activated *Nlrc5*-Deficient Dendritic Cells Is Unaffected despite Partially Reduced MHC Class I Levels

Giorgia Rota,* Kristina Ludigs,* Stefanie Siegert,† Aubry Tardivel,* Leonor Morgado,* Walter Reith,‡ Aude De Gassart,* and Greta Guarda*

NLRC5, a member of the NOD-like receptor (NLR) protein family, has recently been characterized as the master transcriptional regulator of MHCI molecules in lymphocytes, in which it is highly expressed. However, its role in activated dendritic cells (DCs), which are instrumental to initiate T cell responses, remained elusive. We show in this study that, following stimulation of DCs with inflammatory stimuli, not only did NLRC5 level increase, but also its importance in directing MHCI transcription. Despite markedly reduced mRNA and intracellular H2-K levels, we unexpectedly observed nearly normal H2-K surface display in *Nlrc5*$^{-/-}$ DCs. Importantly, this discrepancy between a strong intracellular and a mild surface defect in H2-K levels was observed also in DCs with *H2-K* transcription defects independent of *Nlrc5*. Hence, alongside with demonstrating the importance of NLRC5 in MHCI transcription in activated DCs, we uncover a general mechanism counteracting low MHCI surface expression. In agreement with the decreased amount of neosynthesized MHCI, *Nlrc5*$^{-/-}$ DCs exhibited a defective capacity to display endogenous Ags. However, neither T cell priming by endogenous Ags nor cross-priming ability was substantially affected in activated *Nlrc5*$^{-/-}$ DCs. Altogether, these data show that *Nlrc5* deficiency, despite significantly affecting MHCI transcription and Ag display, is not sufficient to hinder T cell activation, underlining the robustness of the T cell priming process by activated DCs. *The Journal of Immunology*, 2016, 196: 2939–2946.

Antigen presentation to cytotoxic T cells is a powerful immune defense mechanism. For this reason, transcriptional regulation of MHC class I (MHCI) genes is tightly controlled by multiple regulatory motifs. These include an IFN-responsive element, NF-κB binding sites, and a highly conserved regulatory motif known as SXY module, which is proximal to the transcription start site (1). Recent studies led to the discovery of NOD-like receptor (NLR) caspase recruitment domain–containing protein 5 (NLRC5) as the transcriptional regulator occupying the SXY sequence (2–8). NLRC5 does not directly bind the DNA, but it is recruited by the enhanceosome, a DNA-binding complex assembling on the SXY module (2–6). By analogy with CIITA, a thoroughly studied NLR family member that acts as a transcriptional regulator of MHC class II genes, NLRC5 recruits in turn chromatin remodeling and transcription factors, thus orchestrating the transactivation of MHCI genes (9). Thereby, NLRC5 contributes to the transcription of classical (*H2-K* and *H2-D*) and selected nonclassical MHCI genes (2–4, 7, 10).

At steady state, NLRC5 is highly expressed in immune cells and predominantly in lymphocytes; accordingly, its relevance to MHCI transcription is major in lymphoid cells (2, 3, 7, 8, 10). In contrast, in dendritic cells (DCs), which are considered the most efficient APCs, NLRC5 is low and *Nlrc5*-deficient DCs show minor differences in MHCI expression (2, 8, 10). However, activating stimuli such as LPS positively regulate *Nlrc5* transcription in macrophages and DCs, mainly through the autocrine action of type I IFNs (2, 7, 11). This important increase in the levels of NLRC5 raises the possibility that its contribution to MHCI expression augments following DC activation.

Although DCs are the key APCs in most instances, to date, a single study tested the role of NLRC5 in this cell type. The authors observed a defect in OT-I T cell activation using peptide-pulsed, immature *Nlrc5*$^{-/-}$ bone marrow (BM)–derived DCs (BMDCs) (7). Yet, natural routes of Ag presentation by activated DCs, the DCs licensed to stimulate a full-blown T cell response, remain unexplored. We therefore addressed the role of NLRC5 in Ag direct presentation and crosspresentation by activated DCs.

We found that NLRC5 largely contributes to *H2-K* transcription in DCs following exposure to inflammatory stimuli, with *Nlrc5*$^{-/-}$ cells showing a 50% reduction in mRNA and intracellular H2-K levels. Despite that, surface levels of MHCI were only slightly affected. This phenomenon was not restricted to *Nlrc5*-deficient cells, as DCs exhibiting low MHCI intracellular pool due to *Nlrc5*-independent defects showed milder reduction in MHCI surface levels, indicating the existence of a compensatory mechanism salvaging MHCI display. Interestingly, presentation of endogenous Ags by *Nlrc5*$^{-/-}$ BMDCs also exhibited a defect in the range of 50%, indicating that the reduced amount of de novo synthesized MHCI

*Department of Biochemistry, University of Lausanne, 1066 Epalinges, Switzerland; †Ludwig Center for Cancer Research, University of Lausanne, 1066 Epalinges, Switzerland; and ‡Department of Pathology and Immunology, University of Geneva Medical School, 1211 Geneva, Switzerland

Received for publication September 22, 2015. Accepted for publication February 1, 2016.

This work was supported by the Swiss National Science Foundation (PP00P3_139094) and the European Research Council (ERC-2012-StG310890) (to G.G.).

Address correspondence and reprint requests to Prof. Greta Guarda, Department of Biochemistry, University of Lausanne, Chemin des Boveresses 155, 1066 Epalinges, Switzerland. E-mail address: Greta.Guarda@unil.ch

The online version of this article contains supplemental material.

Abbreviations used in this article: BM, bone marrow; BMDC, BM-derived DC; cDC, conventional DC; CTV, CellTrace Violet; DC, dendritic cell; fwd, forward; β_2m, β_2 microglobulin; MHCI, MHC class I; NLR, NOD-like receptor; NLRC5, NOD-like receptor caspase recruitment domain–containing protein 5; poly(I:C), polyinosinic-polycytidylic acid; rev, reverse.

affected the display of intracellular Ags. Despite that, T cell–priming and cross-priming ability by $Nlrc5^{-/-}$ DCs was virtually normal. Taken together, these data indicate that the defects in MHCI transcription and direct Ag presentation observed in activated $Nlrc5^{-/-}$ BMDCs are per se not sufficient to significantly alter priming ability by these cells, highlighting the robustness of this process.

Materials and Methods

Mice

$Rfx5^{-/-}$ (12) and $Rfx5^{+/-}$ littermate controls on a mixed Sv129/C57BL/6 (H2b) background were provided by W. Reith and bred at the University of Geneva (Geneva, Switzerland). *H2-K* hemizygous mice were generated by crossing *H2-K*$^{-/-}$ (13) with C57BL/6 mice in the animal facility of the University of Lausanne. $Nlrc5^{fl/fl}$, $Nlrc5^{-/-}$ (2), *H2-K*$^{+/-}$, β_2 microglobulin $(B_2m)^{-/-}$ (14), OT-I (15), and C57BL/6 were bred in the animal facility of the University of Lausanne and treated in accordance with the Swiss Federal Veterinary Office guidelines.

BMDC differentiation

BMDCs were generated from primary BM, which was isolated by flushing femur and tibia from donor mice. BM was cultured for 7 d in DC differentiation medium (RPMI 1640, 10% FCS, 100 U/ml penicillin, 100 μg/ml streptomycin, 50 μM 2-ME, 10 mM HEPES, supplemented with 20 ng/ml rGM-CSF [ImmunoTools]) in untreated cell culture plates. To enrich for BMDCs, nonadherent cells were transferred into new culture dishes 1 d prior to experiments.

Media and reagents

Lymphocytes were grown in RPMI 1640 supplemented with 10% FCS, 100 U/ml penicillin, 100 μg/ml streptomycin, and 50 μM 2-ME. LPS (100 ng/ml), polyinosinic-polycytidylic acid [poly(I:C)] (100 μg in vivo), and zymosan (10 μg/ml) were purchased from InvivoGen; IFN-β (500 U/ml) from PBL IFN Source; and CpG (2 μg/ml or 20 μg in vivo) from Microsynth. TNF-α (20 ng/ml) and CD40L (1 μg/ml) were provided by P. Schneider (University of Lausanne).

Flow cytometry analysis

For flow cytometry analysis, cells were preincubated with α-CD16/32 (2.4G2) to block Fc receptors and then surface stained for 20 min using Abs against CD3e (145-2C11), CD8a (Ly-2), CD11b (M1/70), CD11c (N418), CD45.1 (A20), CD71 (R17217), CD80 (16-10A1), CD86 (GL1), H2-D^b (28-14-8), H2-K^b (AF6-88.5.5.3), and SIINFEKL H2-K (25D.1.16) (all from eBioscience). Streptavidin conjugated to different fluorophores was from eBioscience. Stainings were performed with appropriate combinations of fluorophores. In some experiments, dead cells were excluded by staining with 10 μg/ml propidium iodide. For analysis of the total (surface and intracellular pool) of MHC molecules, cells were first surface stained, then fixed with 4% paraformaldehyde. After permeabilization with 0.5% saponin in PBS/1% FCS, cells were then stained with Abs to detect MHC levels. Data were acquired with a FACSCanto flow cytometer (BD Biosciences) and analyzed using FlowJo software (Tree Star).

Image stream sample preparation

At least 1×10^6 BMDCs for each condition were analyzed. Cells were preincubated with α-CD16/32 to block Fc receptors and then surface stained with Abs against CD11c and H2-K^b. Then cells were fixed with 4% paraformaldehyde. After permeabilization with 0.5% saponin in PBS/1% FCS, cells were then stained for H2-K^b; to discriminate surface and intracellular signal, anti–H2-K^b Abs coupled with different fluorophores were used. In addition, nuclear (DAPI; Thermo Fischer Scientific) or Golgi (anti-Giantin, ab28039; Abcam) staining was added in selected experiments.

Image stream acquisition and IDEAS analysis

Cells were acquired using Inspire software (Amnis) on a 4-laser 12-channel imaging flow cytometer (Image Stream^X MarkII) using original magnification ×40. Prior to each experiment, the machine was fully calibrated using ASSIST (Amnis). At least 50,000 single cells were acquired/sample, with debris and doublets being excluded based on their area and aspect ratio. Single-stain controls were acquired as required (all channels on, no brightfield and no side scatter image), and a compensation matrix was calculated and applied to the files using IDEAS (v6.1) software. For analysis, cells in focus (using the gradient RMS feature for the brightfield image) and single cells (in a plot using area versus aspect ratio) were gated. Based on DAPI intensity, cells with a sub-G_0 DNA level were excluded. Based on the surface marker CD11c, an erode mask was created to analyze the cell inside. This mask was combined with a CD11c dilate mask using the Boolean operator "AND NOT" to create a cell membrane mask. The intensities of intracellular and extracellular H2-K were calculated in these masks, respectively. To create a mask covering the Golgi apparatus, a threshold mask of 50% in the Golgi image was used. Within this mask, the bright detail similarity of the intracellular H2-K signal was calculated.

Quantitative PCR

RNA extraction, retrotranscription to cDNA, and expression analysis were done, as previously described (4). The following primers were used: NLRC5_forward (fwd), 5′- TGGAGGAGGTCAGTTTGC-3′; NLRC5_reverse (rev), 5′-ATGCTCCTGATTGCTGTGTAG-3′; H2-K_fwd, 5′-TTGAATGGGGAGGAGCTGAT-3′; H2-K_rev, 5′-GCCATGTTGGAGACAGTGGA-3′; Hprt_fwd, 5′-GCAGTACAGCCCCAAAATGG-3′; and Hprt_rev, 5′-AACAAAGTCTGGCCTGTATCC-3′.

H2-K assessment in vivo

H2-K expression was evaluated in lymphocytes (CD3$^+$ cells) or in splenic conventional DCs (cDCs; CD11c^{high}CD11b^{int}) after surface staining or postfixation and permeabilization. In some experiments, mice were i.p. injected with 100 μg poly(I:C) 24 h prior to the analysis.

OT-I cell isolation, labeling, and proliferation analysis

OT-I T cells were isolated with a CD8$^+$ T cell positive isolation kit (Miltenyi Biotec) from spleens of OT-I mice. Enriched CD8$^+$ OT-I cells were then labeled with 5 μM CellTrace Violet (CTV; from Life Tech-

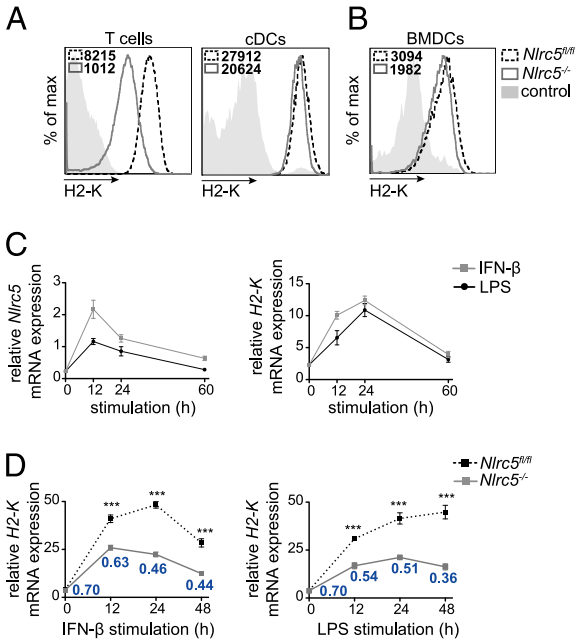

FIGURE 1. *Nlrc5* is upregulated upon inflammatory stimulation and drives *H2-K* transcription in DCs. (**A** and **B**) T lymphocytes (CD3$^+$) and splenic cDCs (CD11c^{high}CD11b^{int}) (A) and BMDCs (CD11c$^+$) (B) from $Nlrc5^{fl/fl}$ and $Nlrc5^{-/-}$ mice were analyzed for surface H2-K expression by flow cytometry. Histograms show a representative example of H2-K fluorescence and mean fluorescence intensity. Results are representative of at least two independent experiments (A and B), with $n = 3$ mice/group (A). (**C**) Wild-type BMDCs were stimulated for 12, 24, or 60 h with IFN-β (500 U/ml) or LPS (100 ng/ml). *H2-K* and *Nlrc5* mRNA expression relative to *Hprt* mRNA were assessed by quantitative PCR. (**D**) $Nlrc5^{fl/fl}$ and $Nlrc5^{-/-}$ BMDCs were stimulated for 12, 24, and 48 h with IFN-β or LPS. Quantitative PCR was performed to assess *H2-K* mRNA expression at each time point (relative to *Hprt* mRNA). Ratios of *H2-K* expression of $Nlrc5^{-/-}$ to $Nlrc5^{fl/fl}$ BMDCs for each time point are indicated in the graph. Results depict mean ± SD ($n = 3$ replicates) (C and D) and are representative of at least two (C) and more than three (D) independent experiments. ***$p <$ 0.001.

nologies) in PBS/1% FCS at 37°C for 20 min. The reaction was quenched with complete medium, and cells were washed and cocultured with the indicated amounts of BMDCs for the described Ag presentation assays in vitro or transferred into the indicated recipient mice to assess cross-presentation in vivo.

Ag presentation assay

For cell-associated Ag crosspresentation, splenocytes of $B_2m^{-/-}$ mice were irradiated with 1,500 cGy, washed, incubated for 10 min at 37°C with 10 mg/ml OVA (purchased from Calbiochem, endotoxins <0.01 EU /μg protein, as tested with Endpoint Chromogenic LAL Assays, Lonza) in complete medium and then washed three times. Cells were then added as immunogen in the indicated numbers to 25,000 BMDCs, cocultured with 50,000 CTV-labeled $CD8^+$ OT-I T cells in a round-bottom 96-well plate. For direct Ag presentation, BMDCs transfected with *GFP* or *GFP-SIINFEKL* mRNA were cocultured in round-bottom 96-well plate at the indicated ratios with 20,000 OT-I T cells. To analyze proliferation dye dilution was assessed by flow cytometer after 48–60 h of culture.

Crosspresentation in vivo

A total of 1.5–2 × 10^6 CTV-labeled congenically marked $CD8^+$ OT-I T cells was transferred i.v. into $Nlrc5^{fl/fl}$ or $Nlrc5^{-/-}$ recipient mice. The day after, mice were immunized in the footpad with 10 μg OVA (purchased from Sigma-Aldrich, endotoxins 0.3 EU/μg protein, as tested with Endpoint Chromogenic LAL Assays, Lonza) and 20 μg CpG. Forty-eight hours later, mice were sacrificed, popliteal lymph nodes were collected, and OT-I T cell proliferation was assessed by flow cytometry.

BMDC transfections

For unstimulated cells, the AMAXA nucleofection protocol specific for immature BMDCs was followed (Lonza). Cells were transfected with 5 nM negative control or 2–5 nM *H2-K* small interfering RNA (Thermo Fischer Scientific) and then stimulated with IFN-β (500 U/ml). For overnight LPS-stimulated cells (100 ng/ml), the AMAXA protocol was optimized using Y-05 program and 2.5 μg in vitro transcribed mRNA encoding for *GFP* or *GFP-SIINFEKL*. Plasmids encoding either for GFP or a fusion protein GFP-SIINFEKL, under the control of the T7 promoter, were provided by P. Pierre (Centre d'Immunologie de Marseille-Luminy, Marseille, France) (16). Plasmids were first linearized with NarI enzyme (NEB) and gel purified (Promega). In vitro transcription was performed with mMESSAGE mMACHINE T7 transcription kit (Thermo Fischer Scientific) following the manufacturer's instructions. mRNA was then purified with RNAeasy mini kit (Qiagen).

Statistical analysis

Statistical analyses were performed using Prism software (GraphPad version 5.0). Differences were calculated with an unpaired, two-tailed Student *t*

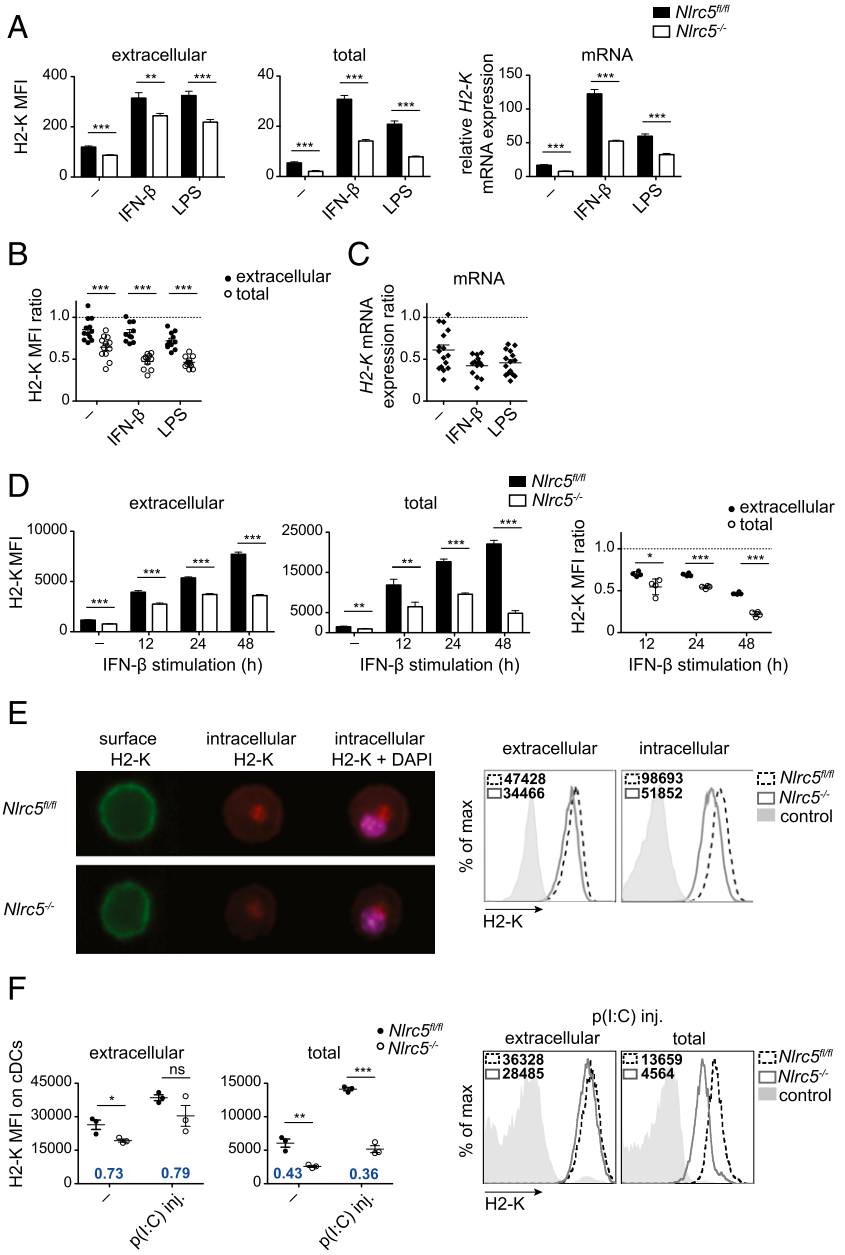

FIGURE 2. *Nlrc5* deficiency affects *H2-K* mRNA and total protein abundance, but mildly surface expression. (**A**) $Nlrc5^{fl/fl}$ and $Nlrc5^{-/-}$ BMDCs were stimulated for 24 h with IFN-β, LPS, or left untreated (−). Mean fluorescence intensity (MFI) of surface and total (following permeabilization) H2-K was evaluated by flow cytometry on $CD11c^+$ BMDCs, whereas *H2-K* mRNA was assessed by quantitative PCR (relative to *Hprt* mRNA). It is important to note that MFI values of surface and total MHCI cannot be directly compared. Results depict mean ± SD (n = 3 replicates) and are representative of more than three independent experiments. (**B** and **C**) Surface, total H2-K, and *H2-K* mRNA were assessed, as in (A). Ratios of MFIs or relative mRNA abundance of $Nlrc5^{-/-}$ to $Nlrc5^{fl/fl}$ were calculated for surface, total protein (B), and *H2-K* transcript abundance (C). Results depict mean ± SEM of 10–12 independent experiments (B) and 13–16 independent experiments (C). (**D**) $Nlrc5^{fl/fl}$ and $Nlrc5^{-/-}$ BMDCs were stimulated for 12, 24, and 48 h with IFN-β or left untreated (−). MFI of surface and total H2-K was evaluated on $CD11c^+$ BMDCs by flow cytometry at the indicated time points. Ratios of MFIs of $Nlrc5^{-/-}$ to $Nlrc5^{fl/fl}$ were calculated for surface and total protein. Results depict mean ± SD (n = 4 replicates) and are representative of more than three independent experiments. (**E**) Representative ImageStream cytometry images of extracellular, intracellular H2-K, and nuclear staining of $CD11c^+$ $Nlrc5^{fl/fl}$ and $Nlrc5^{-/-}$ BMDCs 24 h post-LPS stimulation. Histograms illustrate surface and intracellular H2-K fluorescence on >10,000 events. Results are representative of three independent experiments. Original magnification ×40. (**F**) $Nlrc5^{fl/fl}$ and $Nlrc5^{-/-}$ mice were injected i.p. with 100 μg poly(I:C), or left untreated (−). Splenic cDCs were analyzed 24 h later for surface and total H2-K expression. H2-K MFI values of $Nlrc5^{-/-}$ to $Nlrc5^{fl/fl}$ for extracellular as well as total fluorescence are depicted in the graphs. Histograms show representative examples of surface and total H2-K fluorescence. Results illustrate mean ± SEM (n = 3 mice/group) and are representative of at least two independent experiments. *$p < 0.05$, **$p < 0.01$, ***$p < 0.001$.

test and considered significant when $p < 0.05$ (*), very significant when $p < 0.01$ (**), and highly significant when $p < 0.001$ (***).

Results

NLRC5 significantly contributes to MHCI transcription upon DC activation

Whereas NLRC5 strongly contributes to MHCI expression in lymphocytes, as shown in *Nlrc5*$^{-/-}$ T cells, the defect in cDCs is much milder (Fig. 1A) (4, 10). Similarly, *Nlrc5*$^{-/-}$ BMDCs exhibit only a minor defect in MHCI expression, as depicted in Fig. 1B (8).

However, NLRC5 expression can be increased by inflammatory conditions (2, 7, 11). To explore this possibility in DCs, we assessed the ability of IFN-β and LPS to induce *Nlrc5* and *H2-K* mRNA at different time points following stimulation of wild type BMDCs. Both transcripts increased upon activation, with *Nlrc5* peaking earlier than *H2-K* (Fig. 1C), suggesting that *H2-K* induction is driven by NLRC5. We therefore treated *Nlrc5*$^{-/-}$ and control *Nlrc5*$^{fl/fl}$ BMDCs with IFN-β or LPS and analyzed *H-2K* transcript abundance 12, 24, and 48 h thereafter (Fig. 1D). *H-2K* mRNA levels increased in response to both stimuli, and this was significantly dependent on NLRC5. As also illustrated by the *Nlrc5*$^{-/-}$/*Nlrc5*$^{fl/fl}$ ratio of *H-2K* transcript levels, the contribution of NLRC5 augmented following stimulation (Fig. 1D), compatibly with the kinetics of its upregulation in BMDCs following inflammatory stimulation (2).

Nlrc5$^{-/-}$ *DCs display a mild defect in surface H2-K expression despite significantly reduced intracellular pool*

We next assessed to which extent *Nlrc5* deficiency affected MHCI at the protein level in activated DCs. Unexpectedly, we observed that *Nlrc5*$^{-/-}$ BMDCs exhibited only a moderate alteration of surface H2-K expression 24 h following IFN-β or LPS treatment (Fig. 2A, *left-hand panel*), despite a significant defect of *H2-K* mRNA (Fig. 2A, *right-hand panel*). Interestingly, total levels of mature H2-K (following permeabilization) in *Nlrc5*-deficient BMDCs exhibited a 2-fold reduction as compared with *Nlrc5*$^{fl/fl}$ BMDCs (Fig. 2A, *middle panel*), reflective of the decrease in mRNA. This 2-fold difference in *H2-K* transcript and total protein pool between *Nlrc5*$^{-/-}$ and control BMDCs, and smaller defect in H2-K display, were consistently observed in numerous independent experiments and very prominent upon BMDC activation, as illustrated as ratios of *Nlrc5*$^{-/-}$ to *Nlrc5*$^{fl/fl}$ in Fig. 2B and 2C.

We next analyzed H2-D that, albeit less regulated by NLRC5 (4), showed a trend similar to H2-K (Supplemental Fig. 1A). Conversely, CD71, whose transcriptional regulation is not controlled by NLRC5, was virtually unaltered, underlining the specificity of this phenomenon (Supplemental Fig. 1B). We also found that this compensatory mechanism, partially rescuing H2-K surface expression in *Nlrc5*$^{-/-}$ BMDCs, was common to a range of DC activators, including the innate immune stimuli CpG and zymosan and the cytokines TNF-α and CD40L (Supplemental Fig. 1C). Furthermore, this phenomenon was present 12, 24, as well as 48 h following IFN-β treatment (Fig. 2D). Interestingly, 48 h after stimulation, the defect in total MHCI was striking, translating also in a 2-fold reduction of H2-K display by *Nlrc5*$^{-/-}$ BMDCs (Fig. 2D).

To directly assess intracellular MHCI levels, we took advantage of the ImageStream technology, which combines the statistical power of flow cytometry to the subcellular imagery of microscopy. By specifically quantifying extracellular and intracellular H2-K pools, we confirmed that the latter was strongly affected in LPS-

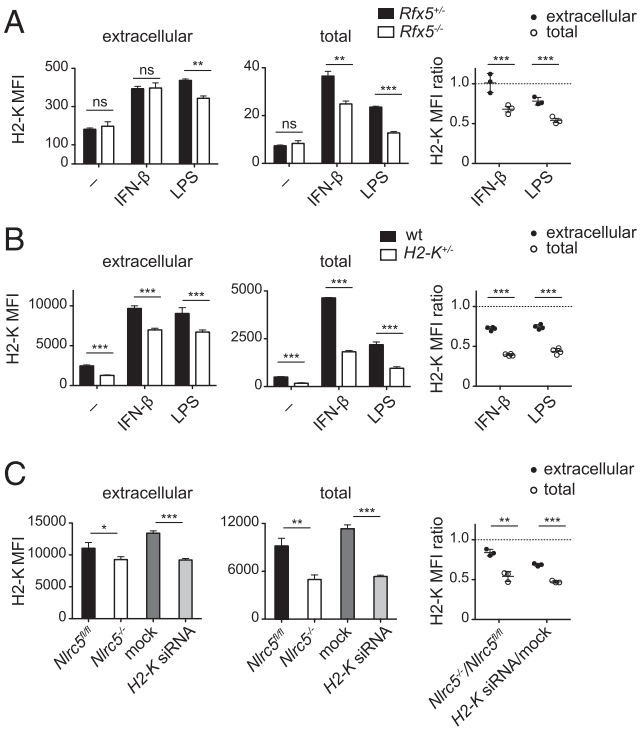

FIGURE 3. A general, NLRC5-independent mechanism compensates H2-K surface levels. (**A**) *Rfx5*$^{+/-}$ and *Rfx5*$^{-/-}$ BMDCs were stimulated with either IFN-β, LPS, or left untreated (−). Mean fluorescence intensities (MFIs) of extracellular and total H2-K were evaluated 24 h poststimulation by flow cytometry on CD11c^{+} BMDCs. Ratios of H2-K MFI values of *Rfx5*$^{-/-}$ to *Rfx5*$^{+/-}$ for extracellular as well as total fluorescence are depicted in the graph. (**B**) Wild type and *H2-K*$^{+/-}$ BMDCs were treated and analyzed as in (A). (**C**) *Nlrc5*$^{fl/fl}$ BMDCs were transfected with either 5 nM negative control small interfering RNA (mock, dark gray bars) or 5 nM *H2-K*–specific small interfering RNA (*H2-K* siRNA, light gray bars). Following transfection, cells were stimulated with IFN-β. In parallel, untransfected *Nlrc5*$^{fl/fl}$ and *Nlrc5*$^{-/-}$ BMDCs stimulated with IFN-β for 24 h were assessed. Surface and total H2-K levels were analyzed on CD11c^{+} BMDCs after 24 h. Ratios of MFI values of *Nlrc5*$^{-/-}$ to *Nlrc5*$^{fl/fl}$ and for *H2-K* small interfering RNA- to mock-transfected cells for extracellular and total fluorescence are illustrated on the *right*. Results represent mean ± SD of $n = 3$ technical replicates (A and C), $n = 4$ technical replicates (B), and are representative of at least two (B) or three (A and C) independent experiments. *$p <$ 0.05, **$p < 0.01$, ***$p < 0.001$.

treated *Nlrc5*$^{-/-}$ BMDCs despite a milder extracellular reduction (Fig. 2E). Of note, mature intracellular MHCI was mainly found in a distinct location, which to a good extent overlapped with the Golgi staining (Supplemental Fig. 1D).

Finally, we tested whether the increase in surface MHCI relative to the intracellular pool observed in *Nlrc5*$^{-/-}$ BMDCs was observed in DCs in vivo. We therefore injected i.p. *Nlrc5*$^{fl/fl}$ and *Nlrc5*$^{-/-}$ mice with poly(I:C), to induce an acute IFN response, and assessed surface and total MHCI levels on splenic cDCs 24 h later. In line with our in vitro results, *Nlrc5*$^{-/-}$ cDCs showed a greater defect in MHCI total pool than surface levels as compared with control cells (Fig. 2F). We therefore identified a phenomenon of altered MHCI distribution, partly uncoupling surface from neosynthesized MHCI pool.

The abundance neosynthesized MHCI fine-tunes its surface levels

We thus asked whether NLRC5 is directly involved in regulating the subcellular distribution of MHCI molecules. Because only a

minority of NLRC5 resides in the nucleus (2), the latter hypothesis could have provided an attractive candidate function for cytoplasmic NLRC5. To uncouple the nuclear from a potential cytosolic function of NLRC5, we analyzed *Rfx5*-deficient BMDCs, which have an intact *Nlrc5* expression (Supplemental Fig. 2A), but lack RFX5, an enhanceosome factor essential for NLRC5 recruitment and transactivation of the MHCI promoter (4–6). Interestingly, IFN-β– and LPS-treated *Rfx5*$^{-/-}$ BMDCs showed H2-K surface expression comparable to control cells, but reduced total protein and mRNA expression, recapitulating results obtained in *Nlrc5*$^{-/-}$ BMDCs (Fig. 3A, Supplemental Fig. 2B). We then decided to assess whether *H2-K*$^{+/-}$ BMDCs, having an expected reduction of H2-K of 50%, presented a similar compensatory mechanism for surface H2-K expression. We observed the predicted reduction of total H2-K levels, whereas surface expression was less strongly affected (Fig. 3B). Finally, we wondered whether a similar phenomenon was observed when H2-K transcription was reduced in a transient manner. We therefore transfected BMDCs derived from *Nlrc5*$^{fl/fl}$ mice with *H2-K*–specific small interfering RNA leading to a partial reduction in *H2-K* transcript abundance (Supplemental Fig. 2C). Again, the reduction in H2-K surface expression was milder as compared with the reduction in total levels (Fig. 3C). Our results highlight that the phenomenon partly uncoupling surface from the neosynthesized MHCI pool originally observed in *Nlrc5*-deficient cells was common to *Nlrc5*-independent models exhibiting low transcript and intracellular MHCI levels.

Nlrc5-deficient DCs are efficient at cross-priming

These results prompted us to test the ability of activated *Nlrc5*$^{-/-}$ BMDCs to prime CD8$^+$ T cells. We started by addressing the ability of *Nlrc5*$^{-/-}$ BMDCs to crosspresent Ags, that is, to display in MHCI molecules of peptides derived from exogenous Ags. To this end, we fed *Nlrc5*$^{-/-}$ and *Nlrc5*$^{fl/fl}$ BMDCs with OVA-coated *B$_2$m*$^{-/-}$ irradiated splenocytes in the presence of IFN-β and cocultured them with transgenic OT-I T cells, which are specific for the H2-K^b–restricted OVA-derived peptide SIINFEKL. As shown in Fig. 4A, T cell proliferation was comparable when induced by *Nlrc5*$^{-/-}$ and *Nlrc5*$^{fl/fl}$ BMDCs.

We next assessed crosspresentation capacity of *Nlrc5*$^{-/-}$ and *Nlrc5*$^{fl/fl}$ DCs in vivo. We adoptively transferred OT-I T cells into *Nlrc5*$^{-/-}$ and *Nlrc5*$^{fl/fl}$ recipients and challenged these animals with the indicated doses of OVA coinjected with CpG. Two days after antigenic challenge, OT-I T cell proliferation was measured in the draining lymph node. As illustrated in Fig. 4B, OT-I T cell proliferation was negligibly affected in *Nlrc5*$^{-/-}$ mice. These data therefore show that *Nlrc5*$^{-/-}$ DCs efficiently cross-prime T cells and suggest that this ability relies on their relatively abundant surface MHCI molecules, compatibly with the sizeable use of recycled molecules for crosspresentation.

Nlrc5 deficiency affects direct Ag presentation, but not T cell–priming ability by DCs

Finally, we analyzed the contribution of NLRC5 to direct Ag presentation, which denotes the display in MHCI molecules of Ags derived from endogenous protein synthesis. To this end, we transfected LPS-treated *Nlrc5*$^{-/-}$ and *Nlrc5*$^{fl/fl}$ BMDCs with mRNA encoding the SIINFEKL peptide and GFP, to select for transfected cells, or GFP only, as control. As shown in Supplemental Fig. 3, similar percentages of GFP$^+$ cells were observed among *Nlrc5*$^{-/-}$ and *Nlrc5*$^{fl/fl}$ BMDCs. We then measured surface H2-K and SIINFEKL-MHCI complex levels on GFP$^+$ cells, as illustrated in Fig. 5A. The net amount of SIINFEKL presented by GFP$^+$ *Nlrc5*$^{-/-}$ DCs was remarkably lower as compared with the levels presented by *Nlrc5*$^{fl/fl}$ BMDCs and relative to surface H2-K, implying a defect in direct Ag presentation.

We next assessed the capacity of these BMDCs to prime OT-I T cells. Despite the defect in the surface level of MHCI loaded with endogenous Ags, the activation of OT-I T cells by transfected LPS-treated *Nlrc5*$^{-/-}$ and *Nlrc5*$^{fl/fl}$ BMDCs was only marginally affected, even at low DC:T ratios (Fig. 5B). As the expression of costimulatory molecules by DCs can strongly amplify TCR-mediated signaling and overcome partial Ag presentation defects (17–19), we measured the expression of CD80 and CD86. Im-

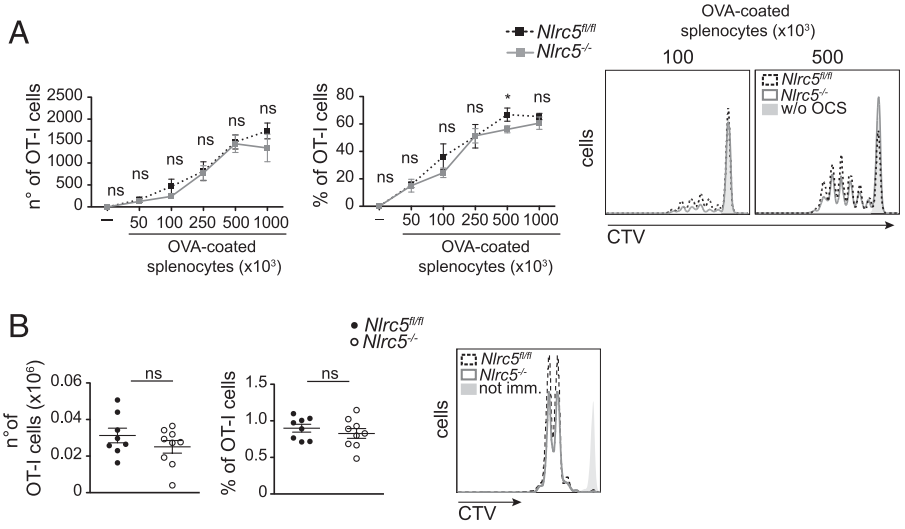

FIGURE 4. *Nlrc5*-deficient DCs efficiently crosspresent exogenous Ags in vitro and in vivo. (**A**) *Nlrc5*$^{fl/fl}$ or *Nlrc5*$^{-/-}$ BMDCs were cocultured with CTV-labeled OT-I T cells and with the indicated numbers of OVA-coated *B$_2$m*$^{-/-}$ irradiated splenocytes (OCS) after 6 h of IFN-β stimulation. Numbers, percentages, and a representative example of OT-I T cell proliferation as observed by flow cytometry after 3 d are illustrated. Results represent mean ± SD (n = 3 technical replicates) and are representative of at least three experiments. (**B**) Proliferation of congenically marked OT-I T cells adoptively transferred into *Nlrc5*$^{fl/fl}$ or *Nlrc5*$^{-/-}$ recipient mice was analyzed in popliteal lymph nodes 48 h after footpad immunization with OVA and CpG. Numbers, percentages, and a representative example of proliferating (CD45.1$^+$) OT-I T cells are depicted. Results are a pool of two independent experiments, illustrate mean ± SEM (n = 8–9), and are representative of at least three independent experiments. *$p < 0.05$.

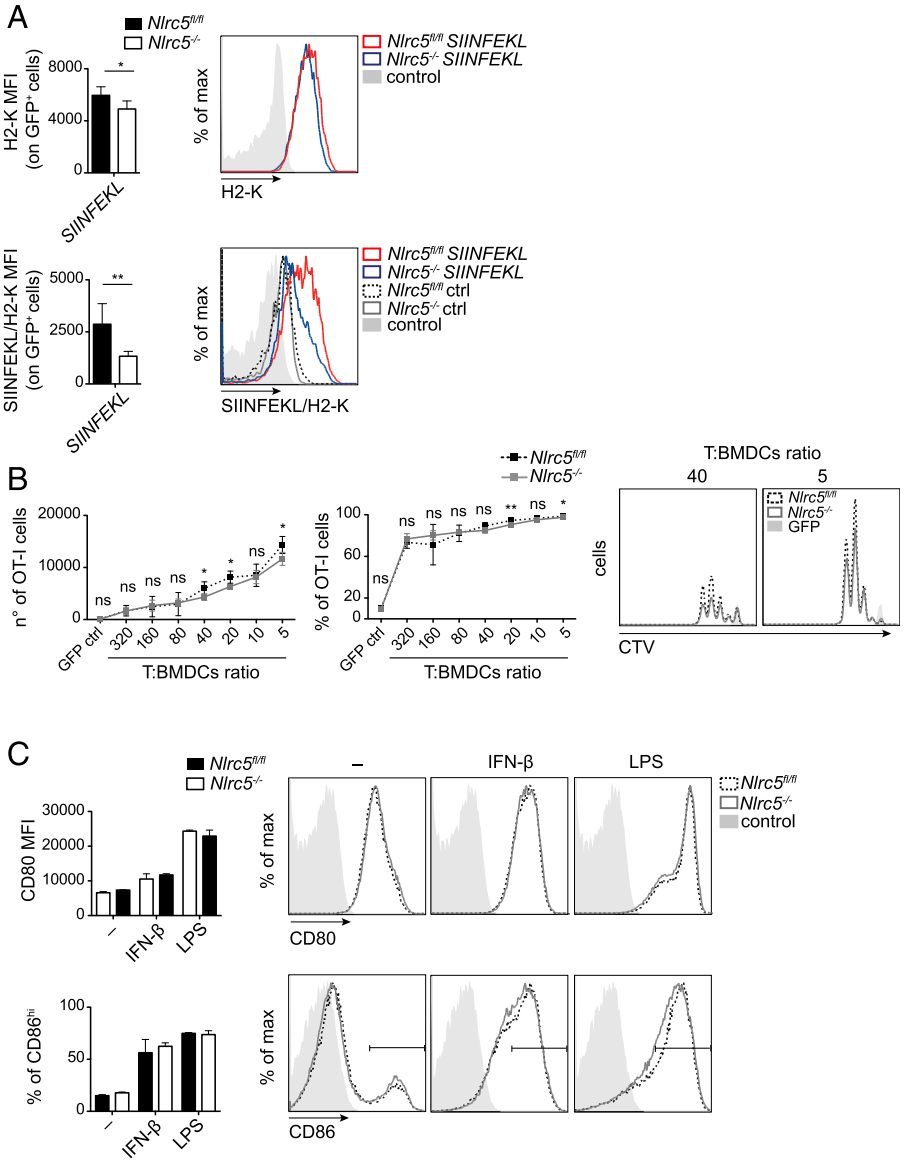

FIGURE 5. *Nlrc5*-deficient DCs are defective in presenting endogenous Ags, but not in T cell priming. (**A** and **B**) *Nlrc5*$^{fl/fl}$ or *Nlrc5*$^{-/-}$ BMDCs were transfected with either *GFP-SIINFEKL* (*SIINFEKL*) or *GFP* control (ctrl) mRNA, as negative control, 12 h post-LPS stimulation. Mean fluorescence intensities (MFI) of H2-K and SIINFEKL-complexed H2-K (SIINFEKL/H2-K) on CD11c^{+} GFP^{+} cells were evaluated 8 h posttransfection by flow cytometry. Histograms on the *right* show representative examples thereof. (B) CTV-labeled OT-I T cells were cocultured 2 d with *Nlrc5*$^{fl/fl}$ or *Nlrc5*$^{-/-}$ BMDCs treated as in (A) with the indicated T cell/BMDCs ratios. Numbers, percentages, and a representative example of OT-I T cell proliferation are depicted. Results represent mean ± SD (n = 5). (A and B) are representative of more than three (A) and two (B) independent experiments. (**C**) MFI of CD80 and percentage of CD86^{high} cells on CD11c^{+} *Nlrc5*$^{fl/fl}$ or *Nlrc5*$^{-/-}$ BMDCs stimulated with IFN-β or LPS for 24 h were assessed by flow cytometry. Histograms show a representative example of CD80 and CD86 fluorescence as detected by FACS. Results represent mean ± SD (n = 4 replicates) and more than three independent experiments (C). $^{*}p < 0.05$, $^{**}p < 0.01$.

portantly, IFN-β– or LPS-treated *Nlrc5*$^{-/-}$ and *Nlrc5*$^{fl/fl}$ BMDCs normally increased costimulatory molecule levels (Fig. 5C). Taken together, these data show that direct Ag presentation is affected in the absence of *Nlrc5*; despite that, T cell activation is robustly induced, suggesting that compensation through costimulatory mechanisms efficiently counteracts weaker TCR-mediated signaling.

Discussion

Even though the importance of NLRC5 as a transcriptional regulator of MHCI in lymphocytes has become increasingly appreciated, its physiological relevance in DCs, the most important APCs in most instances, remained unexplored. Our work demonstrated the importance of NLRC5 in transactivating MHCI genes in DCs following exposure to inflammatory stimuli, which was mirrored in the reduced amount of intracellular MHCI.

Yet, we observed disequilibrium between intracellular and extracellular MHCI distribution in *Nlrc5*$^{-/-}$ as compared with control DCs. This phenomenon was not limited to *Nlrc5*-deficient cells, as we had similar observations in different genetic models presenting a partial defect in MHCI transcription. Therefore, NLRC5 is not directly regulating the subcellular distribution of MHCI, which is rather fine-tuned based on the size of the intracellular MHCI pool. As MHC display is known to be strongly regulated also at posttranslational levels, we can postulate that MHCI trafficking and degradation are controlled through compensatory mechanisms influenced by the intracellular MHCI pool (20–25).

Of note, we observed a dramatic loss of intracellular H2-K molecules and a remarkable decrease in surface levels 2 d after *Nlrc5*$^{-/-}$ DC activation. Even though the contribution by this specific priming condition to the overall immune response in vivo is unlikely to be major, these stimulating data suggest that late priming might be affected by *Nlrc5* deficiency, or that, in the case of infections specifically targeting DCs, defective immunosurveillance by CD8^{+} T cells might ensue.

Among immune cells, DCs are considered the most efficient APCs, and one of the features that mainly distinguishes them is their ability to crosspresent Ags. In our study, *Nlrc5*$^{-/-}$ DCs exhibited efficient cross-priming ability. Whereas we successfully used the Ab specific to SIINFEKL-bound H2-K (clone 25-D1.16) in the context of presentation through the endogenous route (26, 27), we failed to observe a specific staining for the crosspresented epitope. We therefore quantified only DC ability to cross-prime

T cells, what encompasses both Ag display and costimulatory ability (17–19, 27). We therefore speculate that the unaffected costimulatory capacity and the relative abundance of MHCI molecules at the surface of *Nlrc5*$^{-/-}$ DCs, which can feed into the crosspresentation pathway (23, 28), contribute to efficient T cell cross-priming.

In agreement with the reduced levels of MHCI mRNA observed in *Nlrc5*$^{-/-}$ DCs, reduced levels of neosynthesized MHCI molecules were measured intracellularly. Interestingly, the main bolus of mature intracellular MHCI molecules partly overlapped with Golgi staining, lending support to previous observations indicating that this organelle stores the majority of mature MHCI (21). The decrease in *H2-K* mRNA and intracellular pool strongly suggested a reduction of immature H2-K protein in the endoplasmic reticulum, explaining the defective capacity of *Nlrc5*$^{-/-}$ DCs to display endogenous Ags. However, we could not detect significant defects in T cell–priming ability, indicating that the partial reduction observed in Ag-loaded MHCI molecules was amply compensated by costimulatory signals (17–19). It is interesting to notice that, in contrast to the CIITA–MHC class II axis that is silenced upon DC activation by innate immune stimuli (29), NLRC5 and MHCI transcription are induced, thereby actively contributing to direct Ag presentation (2, 7, 11).

Despite being well established and extremely useful, the widely used SIINFEKL-OT-I system has some shortcomings (30). On the one hand, SIINFEKL is an immunodominant epitope, binding H2-K with good affinity, which might thus represent an ideal model for certain microbial epitopes, but not for subdominant ones (31, 32). In contrast, OT-I T cells bear a high-affinity TCR, which well exemplifies the behavior of good-affinity T cell clones (30, 32), but not of low-affinity ones, being potentially impaired in their activation by *Nlrc5*$^{-/-}$ DCs. However, as immunodominant epitopes and high-affinity T cell clones are crucial to most immune responses, we decided in this work to focus on these important aspects.

Our results underline that transcriptional regulation of MHCI is a robust process in DCs, as even the complete loss of NLRC5 only leads to mild or negligible alterations of surface MHCI and priming ability. We can therefore speculate that interindividual variations or immunomodulatory cytokines controlling *NLRC5* or MHCI transcription are unlikely to significantly affect cytotoxic T cell priming, at least for immunodominant epitopes. In light of these findings, it is not surprising that viruses, including Kaposi's sarcoma–associated herpesvirus and HIV, target MHCI at the posttranscriptional level to favor immune evasion (24). Taken together, these data highlight how MHCI-mediated T cell priming is a robust and highly efficient mechanism and how NLRC5 represents one among multiple transcriptional, posttranscriptional, and costimulatory mechanisms that have simultaneously evolved to guarantee this fundamental immune defense process.

Acknowledgments

We thank P. Pierre (Centre d'Immunologie de Marseille-Luminy, Marseille, France), O. Donzé (Adipogen, Lausanne, Switzerland), and P. Schneider (University of Lausanne,) for having contributed tools essential to this project and F. Staehli, Z. Jevnikar, and O. Demaria (University of Lausanne) for technical help.

Disclosures

The authors have no financial conflicts of interest.

References

1. van den Elsen, P. J., T. M. Holling, H. F. Kuipers, and N. van der Stoep. 2004. Transcriptional regulation of antigen presentation. *Curr. Opin. Immunol.* 16: 67–75.
2. Staehli, F., K. Ludigs, L. X. Heinz, Q. Seguín-Estévez, I. Ferrero, M. Braun, K. Schroder, M. Rebsamen, A. Tardivel, C. Mattmann, et al. 2012. NLRC5 deficiency selectively impairs MHC class I-dependent lymphocyte killing by cytotoxic T cells. *J. Immunol.* 188: 3820–3828.
3. Meissner, T. B., A. Li, A. Biswas, K. H. Lee, Y. J. Liu, E. Bayir, D. Iliopoulos, P. J. van den Elsen, and K. S. Kobayashi. 2010. NLR family member NLRC5 is a transcriptional regulator of MHC class I genes. *Proc. Natl. Acad. Sci. USA* 107: 13794–13799.
4. Ludigs, K., Q. Seguín-Estévez, S. Lemeille, I. Ferrero, G. Rota, S. Chelbi, C. Mattmann, H. R. MacDonald, W. Reith, and G. Guarda. 2015. NLRC5 exclusively transactivates MHC class I and related genes through a distinctive SXY module. *PLoS Genet.* 11: e1005088.
5. Meissner, T. B., Y. J. Liu, K. H. Lee, A. Li, A. Biswas, M. C. van Eggermond, P. J. van den Elsen, and K. S. Kobayashi. 2012. NLRC5 cooperates with the RFX transcription factor complex to induce MHC class I gene expression. *J. Immunol.* 188: 4951–4958.
6. Neerincx, A., G. M. Rodriguez, V. Steimle, and T. A. Kufer. 2012. NLRC5 controls basal MHC class I gene expression in an MHC enhanceosome-dependent manner. *J. Immunol.* 188: 4940–4950.
7. Yao, Y., Y. Wang, F. Chen, Y. Huang, S. Zhu, Q. Leng, H. Wang, Y. Shi, and Y. Qian. 2012. NLRC5 regulates MHC class I antigen presentation in host defense against intracellular pathogens. *Cell Res.* 22: 836–847.
8. Biswas, A., T. B. Meissner, T. Kawai, and K. S. Kobayashi. 2012. Cutting edge: impaired MHC class I expression in mice deficient for Nlrc5/class I transactivator. *J. Immunol.* 189: 516–520.
9. Reith, W., S. LeibundGut-Landmann, and J. M. Waldburger. 2005. Regulation of MHC class II gene expression by the class II transactivator. *Nat. Rev. Immunol.* 5: 793–806.
10. Robbins, G. R., A. D. Truax, B. K. Davis, L. Zhang, W. J. Brickey, and J. P. Ting. 2012. Regulation of class I major histocompatibility complex (MHC) by nucleotide-binding domain, leucine-rich repeat-containing (NLR) proteins. *J. Biol. Chem.* 287: 24294–24303.
11. Benko, S., J. G. Magalhaes, D. J. Philpott, and S. E. Girardin. 2010. NLRC5 limits the activation of inflammatory pathways. *J. Immunol.* 185: 1681–1691.
12. Clausen, B. E., J. M. Waldburger, F. Schwenk, E. Barras, B. Mach, K. Rajewsky, I. Förster, and W. Reith. 1998. Residual MHC class II expression on mature dendritic cells and activated B cells in RFX5-deficient mice. *Immunity* 8: 143–155.
13. Pérarnau, B., M. F. Saron, B. Reina San Martin, N. Bervas, H. Ong, M. J. Soloski, A. G. Smith, J. M. Ure, J. E. Gairin, and F. A. Lemonnier. 1999. Single H2Kb, H2Db and double H2KbDb knockout mice: peripheral CD8+ T cell repertoire and anti-lymphocytic choriomeningitis virus cytolytic responses. *Eur. J. Immunol.* 29: 1243–1252.
14. Koller, B. H., P. Marrack, J. W. Kappler, and O. Smithies. 1990. Normal development of mice deficient in beta 2M, MHC class I proteins, and CD8+ T cells. *Science* 248: 1227–1230.
15. Clarke, S. R., M. Barnden, C. Kurts, F. R. Carbone, J. F. Miller, and W. R. Heath. 2000. Characterization of the ovalbumin-specific TCR transgenic line OT-I: MHC elements for positive and negative selection. *Immunol. Cell Biol.* 78: 110–117.
16. Wenger, T., S. Terawaki, V. Camosseto, R. Abdelrassoul, A. Mies, N. Catalan, N. Claudio, G. Clavarino, A. de Gassart, Fde. A. Rigotti, et al. 2012. Autophagy inhibition promotes defective neosynthesized proteins storage in ALIS, and induces redirection toward proteasome processing and MHCI-restricted presentation. *Autophagy* 8: 350–363.
17. Tuosto, L., and O. Acuto. 1998. CD28 affects the earliest signaling events generated by TCR engagement. *Eur. J. Immunol.* 28: 2131–2142.
18. Viola, A., S. Schroeder, Y. Sakakibara, and A. Lanzavecchia. 1999. T lymphocyte costimulation mediated by reorganization of membrane microdomains. *Science* 283: 680–682.
19. McAdam, A. J., A. N. Schweitzer, and A. H. Sharpe. 1998. The role of B7 costimulation in activation and differentiation of CD4+ and CD8+ T cells. *Immunol. Rev.* 165: 231–247.
20. Delamarre, L., H. Holcombe, and I. Mellman. 2003. Presentation of exogenous antigens on major histocompatibility complex (MHC) class I and MHC class II molecules is differentially regulated during dendritic cell maturation. *J. Exp. Med.* 198: 111–122.
21. Ackerman, A. L., and P. Cresswell. 2003. Regulation of MHC class I transport in human dendritic cells and the dendritic-like cell line KG-1. *J. Immunol.* 170: 4178–4188.
22. MacAry, P. A., M. Lindsay, M. A. Scott, J. I. Craig, J. P. Luzio, and P. J. Lehner. 2001. Mobilization of MHC class I molecules from late endosomes to the cell surface following activation of CD34-derived human Langerhans cells. *Proc. Natl. Acad. Sci. USA* 98: 3982–3987.
23. Nair-Gupta, P., A. Baccarini, N. Tung, F. Seyffer, O. Florey, Y. Huang, M. Banerjee, M. Overholtzer, P. A. Roche, R. Tampé, et al. 2014. TLR signals induce phagosomal MHC-I delivery from the endosomal recycling compartment to allow cross-presentation. *Cell* 158: 506–521.
24. Nathan, J. A., and P. J. Lehner. 2009. The trafficking and regulation of membrane receptors by the RING-CH ubiquitin E3 ligases. *Exp. Cell Res.* 315: 1593–1600.
25. Neefjes, J., M. L. Jongsma, P. Paul, and O. Bakke. 2011. Towards a systems understanding of MHC class I and MHC class II antigen presentation. *Nat. Rev. Immunol.* 11: 823–836.
26. Porgador, A., J. W. Yewdell, Y. Deng, J. R. Bennink, and R. N. Germain. 1997. Localization, quantitation, and in situ detection of specific peptide-MHC class I complexes using a monoclonal antibody. *Immunity* 6: 715–726.

27. Nair-Gupta, P., and J. M. Blander. 2013. An updated view of the intracellular mechanisms regulating cross-presentation. *Front. Immunol.* 4: 401.
28. Di Pucchio, T., B. Chatterjee, A. Smed-Sörensen, S. Clayton, A. Palazzo, M. Montes, Y. Xue, I. Mellman, J. Banchereau, and J. E. Connolly. 2008. Direct proteasome-independent cross-presentation of viral antigen by plasmacytoid dendritic cells on major histocompatibility complex class I. *Nat. Immunol.* 9: 551–557.
29. Landmann, S., A. Mühlethaler-Mottet, L. Bernasconi, T. Suter, J. M. Waldburger, K. Masternak, J. F. Arrighi, C. Hauser, A. Fontana, and W. Reith. 2001. Maturation of dendritic cells is accompanied by rapid transcriptional silencing of class II transactivator (CIITA) expression. *J. Exp. Med.* 194: 379–391.
30. Hogquist, K. A., S. C. Jameson, W. R. Heath, J. L. Howard, M. J. Bevan, and F. R. Carbone. 1994. T cell receptor antagonist peptides induce positive selection. *Cell* 76: 17–27.
31. Howarth, M., A. Williams, A. B. Tolstrup, and T. Elliott. 2004. Tapasin enhances MHC class I peptide presentation according to peptide half-life. *Proc. Natl. Acad. Sci. USA* 101: 11737–11742.
32. Hommel, M., and P. D. Hodgkin. 2007. TCR affinity promotes CD8+ T cell expansion by regulating survival. *J. Immunol.* 179: 2250–2260.